This article is a selected paper from the 10th JFPS International Symposium on Fluid Power, Fukuoka, Japan in October 24-27, 2017
JFPS International Journal of Fluid Power System 11-3, 130/135, 2018

Design of a Power Regenerative Hydrostatic Wind Turbine Test Platform*

Biswaranjan Mohanty**, Feng Wang** and Kim A.Stelson **

The demand for community wind turbines is increasing to fulfill local requirements and make the grid more stable. A turbine with a hydrostatic transmission is more reliable and cost effective than a conventional gearbox turbine making it an attractive alternative for community wind turbines. A power regenerative test platform has been built at the University of Minnesota to understand the performance of a hydrostatic transmission in a wind turbine. The design of the test bed is described in detail in this paper. The testbed emulates the rotor torque including the effects of the blade dynamics and pitch in a hardware-in-the-loop configuration. This test platform provides a powerful tool to investigate the performance of new components, controllers, fluids and energy storage methods on the hydrostatic wind turbine transmission.
Keywords: Wind Turbine, Renewable Energy, Hydrostatic Transmission

1. Introduction

The wind energy is the fastest growing green and clean energy source of electricity. The total installed capacity has reached 487 GW by the end of 2016, which is 4.7% of the world's electricity demand [1]. Most wind energy comes from large wind farms. Large wind farms are far away from the point of use, increasing transmission cost. In contrast, small and midsize turbines can fulfil local demand and make the distributed grid more reliable and stable. These distributed wind turbines can be installed in homes, farms, businesses and public facilities such as schools or hospitals to reduce consumer electricity bills.

A conventional turbine uses a multi stage fixed ratio gear box to transmit power from the low speed rotor to the high speed generator. An expensive power converter is used to convert the generator frequency to the grid frequency. Studies conducted by the National Renewable Energy Laboratory (NREL) among others document failure frequency and downtime for wind turbines [2] [3]. The studies show that electrical systems fail frequently with shorter downtimes, but gearboxes and generators fail less frequently with longer downtimes. The failure of gearboxes and generators is due to unsteady wind, causing impact loading which reduces the life of the components. Failures not only decrease the annual energy production of the turbine, but also increase the maintenance cost.

The reliability of a wind turbine can be improved by removing the gearbox. But the downside of the direct drive is it requires permanent magnets, which increases turbine cost and weight. The other way to increase the reliability is by replacing the gear box with a hydrostatic transmission (HST). HSTs are simple, light and cost effective and have high power density. The slight compressibility of the hydraulic fluids in an HST reduces the shock loading on mechanical components increasing their life. An HST is one type of continuous variable transmission, commonly used in off road and construction equipment. HST can be coupled with an accumulator to store energy [4] [5].

Wind energy research and development efforts have primarily benefitted large wind turbines. NREL has dynamometer research facilities to perform steady-state research validation to determine turbine power curves. NREL employs "model-in-the-loop" techniques to emulate rotor, tower, pitch, and yaw systems with 225 kW, 2.5MW and 5 MW dynamometers to test gearbox turbines. The Institute for Fluid Power Drives and Controls in RWTH Aachen University developed a 1 MW hydrostatic wind test platform, designed to replace the commonly used gearbox and power converter [6] [7]. To optimize the transmission efficiency, multiple pumps and motors are used to enable a switching strategy at different wind power inputs. Although a hydrostatic transmission consisting of conventional pumps and motors has lower efficiency than a gearbox, the overall system efficiency is still competitive since the need for a power converter is eliminated.

For the community wind turbine a HST with single pump and motor will be the cost effective and reliable. It is important to understand the performance of the HST under various loading conditions. To measure the performance, a power regenerative hydrostatic wind turbine has been developed at the University of the Minnesota. The design of the testbed is described in this paper.

* Manuscript received January 31st, 2018
** University of Minnesota
(Minneapolis, MN 55455, US)
E-mail: mohan035@umn.edu
*** Zhejiang University
(Hangzhou, Zhejiang 310027, China)

2. Wind Turbine Performance

In a wind turbine, airfoil shaped blades capture kinetic energy from the wind and transform it into rotational energy of the rotor. The rotor power is proportional to the power coefficient (C_p) and the cube of the wind speed (v) as shown in Eq. (1).

$$P_{rot} = C_p(\lambda, \beta)P_{wind} = \frac{1}{2}C_p(\lambda, \beta)\rho A v^3 \qquad (1)$$

$$\lambda = \frac{\omega R}{v} \qquad (2)$$

where ρ is the air density and A is the swept area of the rotor. According to Betz's law, the maximum aerodynamic efficiency of a wind turbine rotor is 59.3% [8]. The power coefficient is a function of the tip speed ratio (TSR) and pitch angle (β), as shown in Eq. (1). The TSR (λ) is the ratio of the blade tip speed to the wind speed, where R is the rotor radius as shown in Eq. (2).

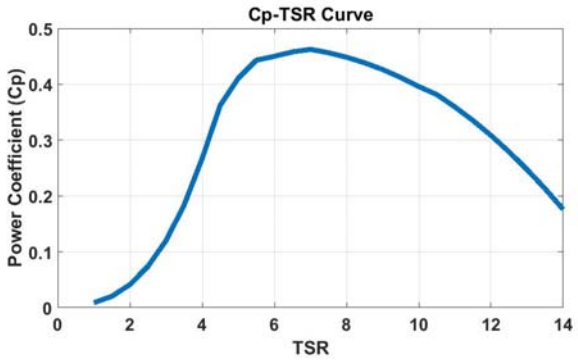

Fig.1 Power coefficient curve of a three bladed variable speed wind turbine

In a wind turbine the rotor interacts with time-varying wind. As a first step, the loading condition of a 90 kW, horizontal-axis and three-bladed variable speed turbine with variable pitch is analyzed. The power coefficient curve of the wind turbine at optimum pitch angle is shown in Fig. 1. The maximum C_p of the rotor is 0.46 at the optimal TSR of 7.

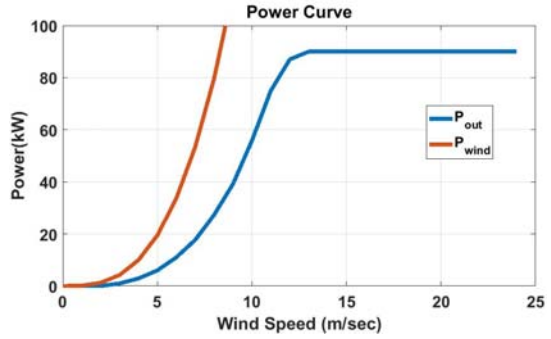

Fig.2 Power curve of a 90 kW wind turbine

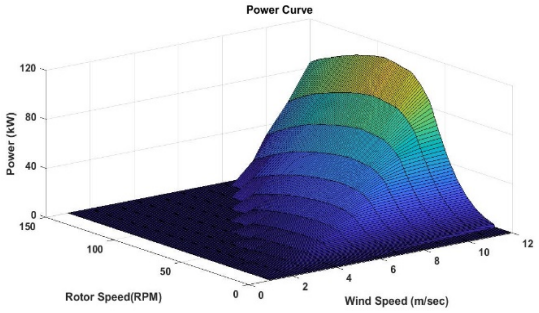

Fig.3 Rotor power curve

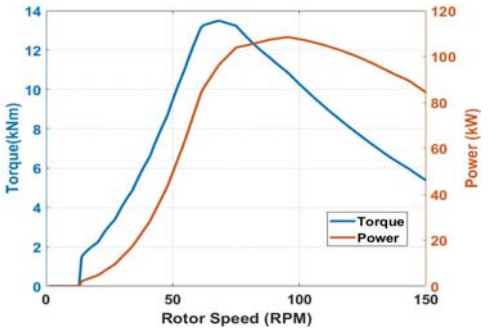

Fig.4 Rotor torque and power at rated speed (12 m/sec)

The output power of the turbine and available wind power is shown in Fig. 2. The turbine output power includes the inefficiency of the drive train. At wind speeds below 3m/sec (cut-in speed), the power available from the wind is less than the turbine losses. At wind speeds above 24m/sec (cut-out speed), the turbine is shut down to avoid damage. In the region from the cut in speed to the rated speed (12m/sec) the turbine is operated at optimal TSR to maximize power. In the region above the rated speed, the power is limited to the rated power by changing the blade pitch.

The rotor power as function of wind speed and rotor speed is plotted in Fig. 3. It can be seen that maximum power at each wind speed is related to an optimal rotational speed. The torque and power at the rated speed is shown in Fig. 4. The rotor power is maximum (108 kW) at the optimal speed of 96 rpm but the torque is a maximum (13.5 kNm) at 67 rpm. This effect has to be taken into consideration during sizing of the hydrostatic transmission.

3. Power Regenerative Test Platform

3.1 Hydrostatic transmission

A hydrostatic transmission consists of a hydraulic pump driving a hydraulic motor. For a continuously variable transmission, at least one unit must have variable displacement. The hydraulic circuit of the transmission neglecting charge pump and cooling circuit is shown in Fig. 5. The rotor drives the fixed displacement pump and the variable displacement motor drives the generator. This choice takes advantage of commercially available hydraulic components, control simplicity, transmission efficiency and cost, and is therefore the most practical solution. The closed circuit HST is chosen, eliminating the need for a bulky reservoir, making the transmission more compact.

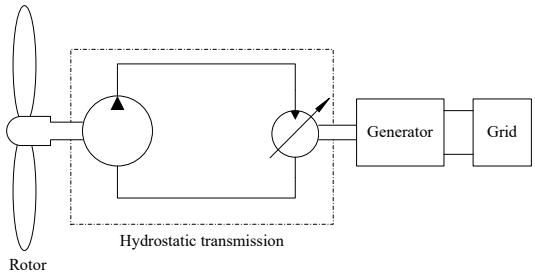

Fig.5 Schematic of HST wind turbine

The output pressure (p) of the pump is directly proportional to the applied torque (T), as shown in Eq. 3. Where D_p is the displacement of the pump in cc/rev.

$$T = \frac{pD_p}{2\pi} \tag{3}$$

Based on the rotor torque shown in Fig. 4 and the maximum pressure of the pump (350 bar), a 2512 cc/rev Hägglunds radial piston pump was selected. The large displacement pump is suitable for low speed and high torque application.

The HST decouples the generator speed from the rotor speed, allowing the generator to run at synchronous speed (1800 rpm) with time varying wind speeds. This also eliminates expensive power converters. The hydraulic motor converts the hydraulic flow (Q) to match the synchronous speed of the generator (ω_g).

$$Q = \omega_r D_p = \omega_g x D_m \tag{4}$$

As shown in Eq. (4), the ratio of rotor speed (ω_r) to generator speed is proportional to the displacement ratio. D_m is the full displacement of the motor and x is the fraction of displacement. A 135cc/rev variable displacement axial piston motor was selected to operate the motor at full displacement at optimal rotor speed.

In the HST, there are fluid losses through the components. To make up the case drain and leakage losses a charge pump is added to the circuit. Assuming a 75 percent volumetric efficiency of the HST, a 36cc/rev fixed displacement gear pump has been used in the charge circuit. The mechanical losses of the transmission heat up the hydraulic fluid. A cooling system is added to the HST to draw heat from the fluid. Assuming a 70 percent mechanical efficiency of the HST, 30 kW of heat needs to be removed for a 100 kW system. A shell and tube type, water cooling 40kW heat exchanger has been installed.

3.2 Test Platform

The power regenerative research platform consists of two closed loop hydrostatic circuits as shown in Fig. 6. The block in dark gray is the hydrostatic transmission under investigation as described above. The block in light gray is the hydrostatic drive (HSD), to simulate the rotor driven by time-varying wind. The output power of the HSD is fed to the pump of the HST through the rotor. The rotor is supported by two spherical roller bearings and the motor and pump are mounted

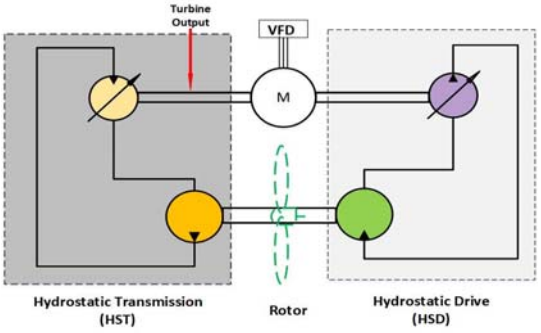

Fig.6 Schematic of power regenerative test platform

on the splines of the shaft. The assembly is shown in Fig. 7.

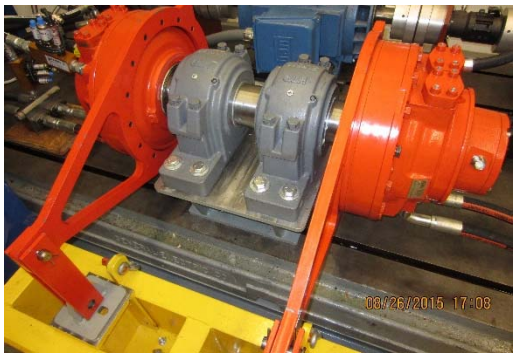

Fig.7 Rotor assembly

The rotation of the hydraulic pump and the motor are restricted by the torque arms.

The HSD consists of an axial piston variable displacement pump (180cc/rev) and a large fixed displacement radial piston motor (2512cc/rev). The pump has an integrated internal charge pump to make up for the volumetric losses in the HSD circuit.

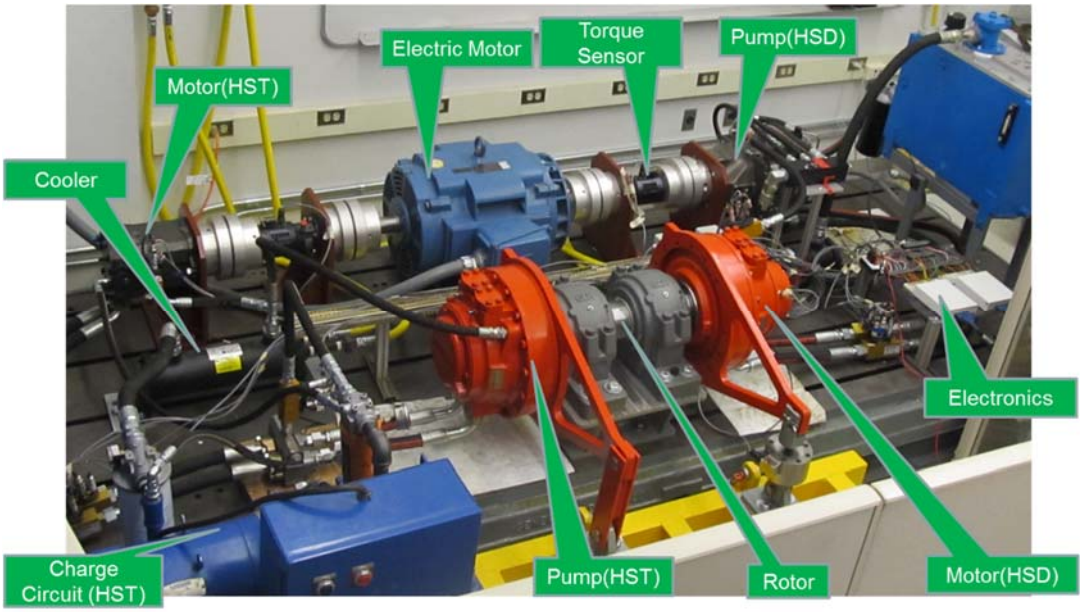

Fig.8 Power regenerative test platform

The inertia of the rotor has a considerable effect on the dynamic behavior of the turbine. It is not practically possible to install a large flywheel on the test platform. As a result, the rotor on the test platform has significantly lower inertia than the rotor in the real turbine. To simulate the real dynamics of the rotor of a turbine, it is necessary to consider effect of large blade inertia in the control of the research platform. This can be done by introducing a modified input torque (τ_d) of the low speed shaft (J_s) to compensate for the effect of the large inertia. The modified torque of the rotor is given by

$$\tau_d = \tau_r - (J_r - J_s)\dot{\omega}_r \qquad (5)$$

Where τ_r is the rotor torque of the actual turbine, J_r and J_s are the moment of inertia of actual rotor and testbed rotor. The modified aerodynamic torque (τ_d) is simulated by controlling the line pressure in the HSD, by changing the displacement of the variable motor. The tracking of the torque/pressure will be performed by a feedback controller.

Instead of dissipating the turbine output power, the power is fed to the HSD along with electric power, allowing power regeneration. Assuming 80% overall efficiency of HST and HSD each, a total of 55 kW of power losses in the circuit is compensated by the electric motor. A three phase, four pole, squirrel cage induction motor with synchronous speed of 1800 rpm (120f/p) is mounted on the high speed shaft, between the pump of the HSD circuit and the motor of the HST circuit. The Variable Frequency Drive (VFD) of the electric motor is set to control the high speed shaft at constant synchronous speed. This enables the test stand to operate with less electric power and eliminates the use of resistors as the load. The power regenerative test platform is shown in Fig. 8. The HST and HSD loops of the test platform have independent hydraulic circuits so that fluid in each circuit can be varied. Each circuit is equipped with a suction and a return line filters to clean the oil and an independent oil cooler to control the oil temperature.

3.3 Sensors and Data Acquisition

The test platform is equipped with 27 sensors to monitor the system performance and three analog inputs to control the displacement of the HST motor, the displacement of the HSD pump and the speed of the electric motor. The pump and motor displacement are controlled by adjusting the swash plate angle with a solenoid valve requiring 225-600 mA for the HST motor and 280-740 mA for the HSD pump. The DAQ cannot provide the high currents required for the swashplate solenoid, so to precisely control the swash plate angle an electronic valve control (EVC) is used. The EVC can be used in simple proportional single coil or dual-coil applications even for more complex closed-loop pressure/speed control. The EVC is configured by its own graphical user interface for two independent single coil operation with a PWM frequency of 100 Hz for each coil. The power to the EVC is supplied

independently to eradicate noise of 100Hz and its harmonic frequency in other sensors.

The speed of the electric motor is controlled by the VFD by varying the input frequency and voltage. The VFD chops the signal at 4 kHz for desired frequency and voltage. Input command of 0-10 VDC is supplied from the DAQ to control the electric motor speed from 0-1800 RPM.

The rotor shaft speed is measured with a speed encoder mounted at the end of the shaft. Rotational speed sensing unit, Hägglunds SPDC, is a digital incremental encoder using magnetic sensing. The sensor generates two square wave signals with 90° phase shift for detection of speed and direction of rotation. For connection, the F/A Converter converts a single pulse train to a 4-20 mA output signal. The output is based on an internal reference frequency selectable in 16 steps and connected to the DAQ board.

The rotor torque (τ_r) is calculated from the force (F) measured on the load cell with torque arm of distance (d) 0.6m. The size of load cell is calculated by the equation given below.

$$\tau_r = Fd = \frac{pD_p}{2\pi\eta_{mp}} \tag{6}$$

The system is designed for 350 bar pressure (p). Assuming 90% mechanical efficiency (η_{mp}) of the fixed displacement motor (2512 cc), the maximum force on the load cell is 26 kN. A load cell of a capacity of 33 kN is installed to measure the force as shown in Fig. 9. The 3mV/V load cell output is amplified with an inline amplifier to 0-10 VDC.

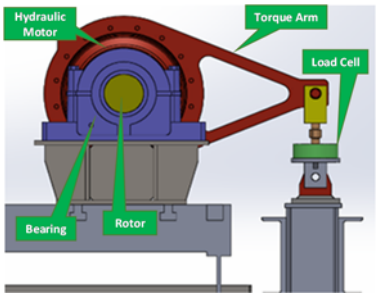

Fig.9 Load cell assembly

Fig.10 Flow sensor module

The Activa Sensor Array module consisting of pressure, temperature and flow sensors is mounted in line with the high pressure and low pressure lines of the HSD and HST as well as the return lines of the HST to monitor the performance of each component. This compact unit is shown in Fig. 10. It requires only one hydraulic line break. The module has a turbine type flow sensor with an analog output of 0-5 VDC. The pressure and temperature sensors generate 4-20 mA analog signal outputs.

In the high speed shaft, two rotary torque sensors were installed to measure the torque and speed. One is mounted between the electric motor and the HSD pump and the other is mounted between the HST motor and the electric motor. The rotary torque sensor is shown in Fig. 11.

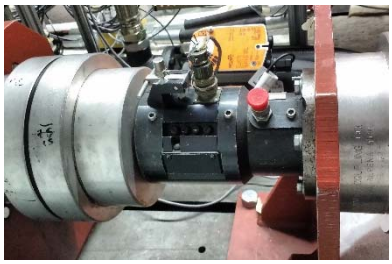

Fig.11 Rotary torque sensor

The sensitivity of the torque sensor is 4 mV/volt, which is prone to noise. Thus, this signal requires a transducer inline amplifier. The 4 kHz chopping frequency of the VFD makes the torque signal distorted due to aliasing. The signal was analyzed by using an oscilloscope. The Fast Fourier Transform (FFT) spectrum of the signal is shown in Fig. 12. An active, multiple feedback, low pass Butterworth filter was designed with cutoff frequency of 100 Hz. The performance of the filter was compared with the Bode plot of the transfer function as shown in Fig. 13. The torque sensor is integrated with 60 toothed gear and a magnetic pick up sensor to measure the shaft speed.

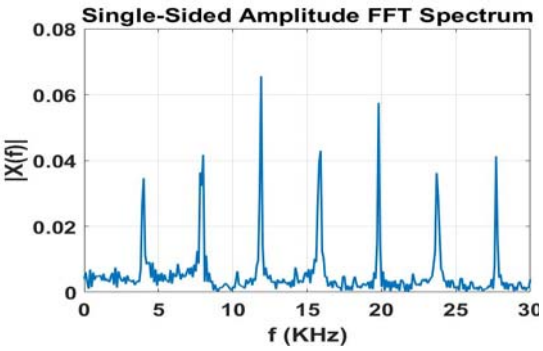

Fig.12 FFT spectrum of the unfiltered torque signal

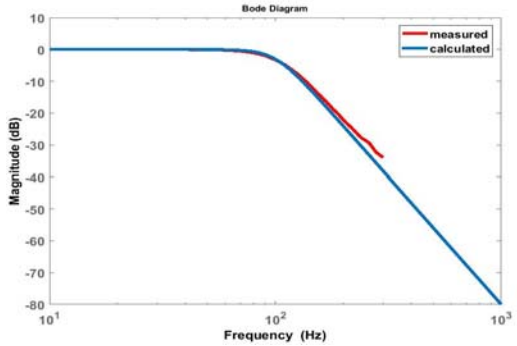

Fig.13 Frequency response of a Butterworth filter

Analog voltage and current signals from all sensors are collected by two terminal boards. The 4-20 mA analog current signal is converted to 0-10 VDC by using a 500 ohm resistor. The noise from environmental electromagnetic interference was avoided by using shielded and twisted pair cables. To avoid ground loops, a single ground was created for all sensors and supply line. There is a common supply of 24 volts for all sensors.

The signals from the sensors are sampled by the DAQ, which converts the analog signal to digital numerical values that can easily be read by a computer. A NI-6259 DAQ, from National Instrument is used for the testbed. It is a high-speed multifunction M Series DAQ board designed for PCI slot with 32 analog inputs and 4 digital outputs at 16 bit resolution. Each analog input is capable of capturing two types of signals: voltages ($\pm 5, \pm 10V$) and currents ($0 - 20mA$). The NI 6259 is connected to the PCI slot which is located in the target computer. Then two cables from the NI 6259 divide the channels and connect to the terminal boards. The two terminal boards collect all the signals from the sensors. In a DAQ, a multiplexer switches from one channel to the next to read the signal. High source impedance on a scanned channel causes its settling time to increase and hence reads the previous channel data. This is called the ghosting effect. To avoid ghosting and crosstalk the multiplexing frequency was decreased to 100 kHz.

Matlab xPC target is used to execute a Simulink model on the target computer for fast prototyping, hardware-in-the-loop (HIL), and other real-time testing applications. xPC Target is a real-time software environment from MathWorks that can manipulate several separate workstations at one time. It also transfers data back to the host machine while reading inputs and issuing commands to the data acquisition boards. The xPC target allow us to employ model-in-the-loop techniques to emulate rotor torque by considering blade aerodynamics and blade pitch. It also allow us to implement a real time control strategy on the testbed.

4. Conclusion

The design of a power regenerative hydrostatic test bed is described in this paper. This test bed allow us to test the performance of the hydrostatic transmission at different wind conditions. Test bed is equipped with sensors to monitor the system behavior. The testbed can emulate rotor torque of 14 kNm which is equivalent to a 100 kW rotor power turbine. This test platform provides a powerful tool to investigate the performance of the new components, controllers, fluids and energy storage method on the hydrostatic wind turbine transmission.

Acknowledgments

This project is funded by the National Science Foundation under grant #1634396.We also thank Eaton, Linde, Danfoss, Bosch Rexroth, Flo-tech and ExxonMobil for donating the components for the test bed. We are thankful to Ching-Sung Wang, a visiting scholar from National Taiwan University, for working on the data acquisition and control system for the test platform.

References

1) World wind energy association report, www.wwindea.org
2) Sheng, S.: Report on wind turbine subsystem reliability- a survey of various databases. National Renewable Energy Laboratory, Golden, CO, *Tech. Rep. NREL/PR-5000-59111*, 2013.
3) Lange,M.,Wilkinson,M.,and Delft,T.,T.V.: Wind turbine reliability analysis. DEWEC, Bremen, 2011.
4) Thul,B.,Dutta, R., Stelson, K. A.:Hydrostatic transmission for mid-sized wind turbines, 52nd National Conference on Fluid Power, Las Vegas, USA, 2011.
5) Dutta,R.,Wang,F., Bohlmann,B.F., Stelson,K.A.: Analysis of short-term energy storage for midsize hydrostatic wind turbine. Journal of Dynamic Systems, Measurement, and Control. Vol.136,No.1,011007(2014)
6) Schmitz,J.,Vatheuer, N., Murrenhoff,H.: Hydrostatic drive train in wind energy plants. RWTH Aachen University, IFAS Aachen, Germany. 2011 Mar 14.
7) Schmitz,J.,Diepeveen,N.,Vatheuer,N.,Murrenhoff,H.: Dynamic transmission response of a hydrostatic transmission measured on a test bench. EWEA; 2012 Dec 31.
8) Betz A. Introduction to the theory of flow machines; 1966.